IFAC Journal of Systems and Control 31 (2025) 100297

Contents lists available at ScienceDirect

IFAC Journal of Systems and Control

journal homepage: www.elsevier.com/locate/ifacsc

Full length article

A top-down approach for climate change mitigation strategies

Claudio Marchesi, Michele Francesco Arrighini *, Laura Zecchi, Marialuisa Volta

Department of Mechanical and Industrial Engineering, University of Brescia, Brescia, 25123, Italy

ARTICLE INFO

Article history:
Received 23 July 2024
Received in revised form 24 January 2025
Accepted 29 January 2025
Available online 3 February 2025

Keywords:
Climate change
Air quality
IAM
Carbon dioxide
Optimization

ABSTRACT

This research examined the effects of various GHG reduction policies on climate change via optimization techniques using a top-down approach. The aim was to examine how different aspects of policies to reduce CO_2 and CH_4 emissions would affect changes in temperature compared to pre-industrial levels from 2025 to 2100. The proposed top-down approach allows for the investigation of several factors that may influence the results: (i) the objective function, (ii) the reduction pathway, and (iii) the starting point of the optimization. Two different objective functions were minimized: the overall sum of the temperature between 2025–2100 and the value at 2100. The results were also compared in terms of the reduction trajectories: two different emission trends were assumed: a gradual (gaussian) fall in emissions or a fast (exponential) decline, starting in 2025, in 2030, and in 2035. The mitigation of greenhouse gas (GHG) emissions was limited to a certain range of scenarios outlined by the Intergovernmental Panel on Climate Change (IPCC). These scenarios were determined by analyzing economic, social, and technical developments expected to occur in the next few decades. The analysis also included the interaction in global warming of air pollutant emission variations due to climate policies. The results revealed that exponential trajectories, depending on the initial year, can facilitate the stabilization of global temperatures below 1.5 °C. In contrast, gaussian trajectories were more likely to overtake this threshold if implementation is delayed beyond 2025.

1. Introduction

Climate change is a global phenomenon that has significant consequences for various aspects of the environment, society, and human health. Along with air quality issues, climate change poses risks to individuals, communities, economies, and ecosystems (Anenberg, Dutton, Goulet, Swain, & van der Pluijm, 2019).

Even now, climate change has consequences, particularly for vulnerable populations and developing countries. The consequences are not limited to specific regions or sectors but have global implications. Climate change can affect international relations, migration patterns, and geopolitical stability (Eghweree & Imuetinyan, 2019). It is closely linked to human activities, such as the burning of fossil fuels, agriculture, and industrial processes, which release significant amounts of greenhouse gases (GHGs) into the atmosphere, including carbon dioxide (CO_2), methane (CH_4), and nitrous oxide (N_2O) (Saunois et al., 2020). These GHGs act as a blanket, trapping heat in the Earth's atmosphere and increasing the greenhouse effect, which origins to global warming and climate change (Sherwood et al., 2020). Understanding the relationship between climate change, human activities, and GHG emissions is crucial for developing effective mitigation strategies to tackle the challenge.

According to that, most nations worldwide approved the Paris Agreement in December 2015, entered in to force on 4 November 2016 (Delbeke, Runge-Metzger, Slingenberg, & Werksman, 2019). The primary objective is to implement collaborative measures to limit the global temperature anomaly, defined as the difference between the annual average temperature and the average temperature observed from pre-industrial era, with the ambitious target of limiting this increase to 1.5 °C. Within this context, the use of suitable modeling tools may support decision-makers in designing efficient control techniques to address the problem. Integrated Assessment Models (IAMs) are valuable instruments for understanding the complex interactions of the system as they examine how economic activities, energy management, land use, emissions, and climate change are connected to each other, making them a fundamental in climate policy studies (Ackerman, DeCanio, Howarth, & Sheeran, 2009; Duan, Zhang, Wang, & Fan, 2019). This approach maximizes the utility function varying anthropogenic GHGs emissions across various sectors from a bottom-up perspective, constrained to different assumptions in demography, human development, economics and lifestyle, policies and institutions, technology, environment, and natural resources. Some of the IAMs that provided mitigation strategies include a process-based description of the land system in addition to the energy system (Hasegawa, Fujimori, Ito,

* Corresponding author.
E-mail addresses: claudio.marchesi@unibs.it (C. Marchesi), michele.arrighini@unibs.it (M.F. Arrighini), laura.zecchi@unibs.it (L. Zecchi), marialuisa.volta@unibs.it (M. Volta).

https://doi.org/10.1016/j.ifacsc.2025.100297

Takahashi, & Masui, 2017; Howells et al., 2013), and a certain number have been extended to include air pollutants (Rafaj et al., 2021), and water use (Fricko et al., 2016; Hejazi et al., 2014; Mouratiadou et al., 2016).

In the IPCC Special Report on Global Warming of 1.5 °C (Masson-Delmotte et al., 2018) pathways for CO_2 emission reductions are presented, specifically showing linear trajectories that achieve net-zero emissions by 2040 to align with the 1.5 °C target, and they are constructed with a top-down approach without any socio-economic assumptions. However, in the later chapters of the report, the IPCC assesses more detailed scenarios for limiting global warming, constructed with a bottom-up approach in which emissions emerge as a result of socio-economic trajectories, technological advances and policy interventions.

In this research a decision problem based on a top-down approach was proposed, which aimed to minimize the temperature anomaly by changing the CO_2 and CH_4 global emissions from 2025 to 2100. The top-down approach in this context focuses on optimizing global emissions directly as decision variables, providing a high-level perspective on the aggregate mitigation effort required to achieve the temperature target. These emissions were constrained to the Illustrative Mitigation Pathways (IMPs) defined by the IPCC. These pathways represent a range of emission scenarios derived from socioeconomic, technological, and policy developments that demonstrate how different trajectories can effectively limit global temperature rise to below 2 °C or 1.5 °C (Shukla et al., 2023). Unlike the bottom-up method that identifies the optimal combination of actions or policies maximizing the economic utility, the top-down approach proposed in this paper allows the analysis of several policy elements, including:

- Reduction propensity: two functions that describe the reduction in GHG emissions were considered: a gaussian function representing a gradual decay and an exponential function reflecting a more drastic decrease. This analysis enabled to assess the effectiveness and feasibility of different reduction strategies.
- Objective Function: two objective functions were considered. The total sum of all temperatures from 2025 to 2100, and only the temperature anomaly at 2100.
- The starting – year: by varying the starting point of the optimization, the impact on temperature anomalies at the end of the century was evaluated. The baseline scenario considered 2025 as a starting point.

Furthermore, the research considered that the GHG emission reduction measures also imply traditional air pollutants emission reductions. The link between CO_2 and traditional pollutant emissions i.e., sulfur oxides (SO_x), non-methane volatile organic compounds (NMVOC), nitrogen oxides (NO_x), and particulate matter (PM) was employed via a curve-fitting functional approach. The same was carried out for ammonia (NH_3) in relation to CH_4. The link between GHG emissions and temperature anomalies was described by the Finite Amplitude Impulse Response climate model (FaIR v1.3) (Leach et al., 2021; Smith et al., 2018).

2. Materials and methods

2.1. The decision problem

In this paragraph, the formulation of the optimization problem is reported. The decision problem was investigated as a single-objective function optimization with the goal of minimizing the temperature anomaly related to 1765, the pre-industrial era. The global emissions of CO_2 and CH_4 from 2025 to 2100 were considered as the decision variables, where the IPCC reference scenarios from AR6 (IMPs) serve as constraints. According to the proposed approach, different decision problems were considered depending on the type of objective function, the choice of function for GHG emission reduction, and the starting year of the optimization. The scheme of the decision problem is summarized in Fig. 1. Starting with a given value of temperature, the optimizer found a solution to the decision problem, i.e., the function parameters, and a new set of GHG emissions was calculated. A simple climate model, the FaIR model, received as inputs the new set of CO_2 and CH_4 emissions and the new emissions of non-GHG species calculated with the functional approach described above. The FaIR model calculated the new temperature, and the process was repeated until convergence. Traditional pollutants, while not treated as decision variables, exerted significant influence on the optimization framework. Their inclusion aimed to account for their indirect effects on temperature outcomes, impacting temperature projections throughout process execution.

2.1.1. Objective function

The problem was posed as follows:

$$\min_E \{F(E)\} = \min_E J(E) \tag{1}$$

Where E represents the worldwide emissions of CO_2 and CH_4, and $J(E)$ is the objective function taken as the sum of temperatures from the initial year to 2100 or as a single value at 2100.

Therefore, two decision problems were considered: minimize the total sum of the temperature anomalies:

$$\min_E \{F_1(E)\} = \min_E \left\{ \sum_{i=t_0}^{2100} T_i(E) \right\} \tag{2}$$

and minimize the temperature anomaly at year 2100

$$\min_E \{F_2(E)\} = \min_E \{T_{2100}(E)\} \tag{3}$$

where:

- t_0 is the starting point of the optimization, set to 2025 as the baseline optimization.
- T_i is the temperature anomaly related to the pre-industrial era (year 1765) at the year i.

In the first case, the objective of minimizing the sum of the temperature anomalies was to limit the possibility of transitory temperature increases in the interval. This strategy takes into account the cumulative impact of emissions over a period of time, effectively managing the total rise in temperature. On the other hand, where only the temperature at the end of the century was minimized, there may be a potential impact on the temperature transient increase. Focusing simply on a single value of temperature could miss the temporary variations in temperature that result from fluctuating emission patterns over the course of the century.

2.1.2. Decision variables

Two different mathematical functions, namely gaussian and exponential, were used to describe emission trajectories to solve (1). Considering the starting point at 2025, a total of four decision problems were investigated, assuming that CO_2 and CH_4 emissions will follow gaussian or exponential reduction pathways. The decision variables are, therefore, each function's parameters. The gaussian function, distinguished by its bell-shape, represents a progressive decrease in emissions over time. This gradual reduction implies a smoother change in emission patterns, allowing more manageable adaptations in social and industrial practices. On the other hand, the exponential function exhibits a rapid decrease from the beginning, resulting in a more incisive policy to reduce emissions.

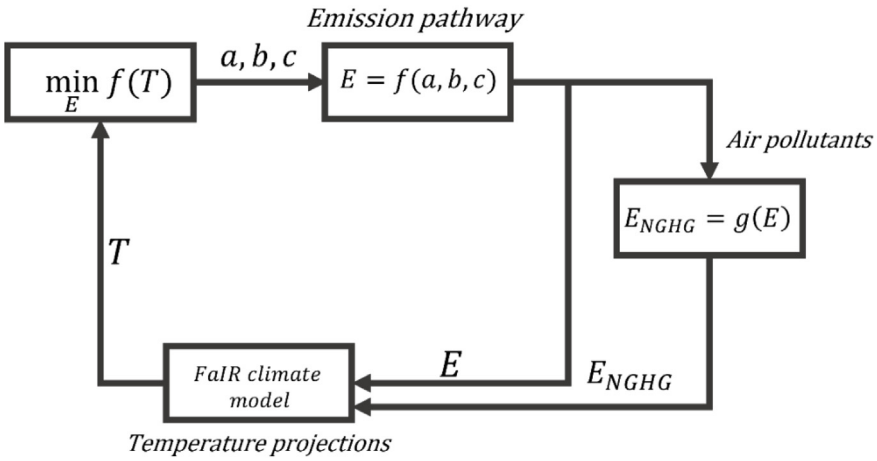

Fig. 1. Data flow scheme of the decision problem.

This approach aimed to explore the propensity of reducing GHG emissions for climate change mitigation.

In the first scenario, fossil CO_2 and CH_4 were modeled as follows:

$$E_{i,j} = a_j e^{-\frac{(i-c_j)^2}{b_j}} + d_j \tag{4}$$

where i represents the year and j represents the considered GHG, respectively. In the gaussian curve, a indicates the amplitude, b represents the breadth of the curve, and c corresponds to the year of peak emission. The offset parameter d was restricted to explicitly include carbon capture and storage (CCS) methods with respect to CO_2 emissions. The capture of methane was not taken into account and the offset was set to zero before the optimization process.

The second function selected represents a strong decrease in emissions over time:

$$E_{i,j} = f_j e^{-\frac{(i-t_0)}{g_j}} + h_j \tag{5}$$

Here f denotes the magnitude, g indicates the timeframe of the exponential trend, and h accounts for CCS.

Prior to 2025, a set of emissions from 1765 (the pre-industrial era) was adopted. The emissions correspond to SSP2-4.5 middle-of-the road pathway (Riahi et al., 2017). The database was obtained from the Climate Model Intercomparison Project 6 (CMIP6) (Nicholls et al., 2020), where data were available only at decade intervals. The annual emissions between consecutive years were estimated via linear interpolation.

2.1.3. Constraints

Two different types of constraints were considered for the decision problem: those ensuring continuity and adherence to specified emission levels and bound constraints defining the feasible solution space based on economic, technical, and social considerations evaluated by the IPCC.

Eqs. (3) and (4) were subjected to

− starting point emission equal to SSP2-4.5:

$$E_{t_0,j} = E_{t_0,ssp_j} \tag{6}$$

Constraint (6) fixed that the GHG emission at the starting point of the optimization was equal to the emission value of the middle-of-the-road scenario, ensuring continuity in the emission pathways.

Furthermore, the gaussian function (3) was also subjected to

− first order constraint for continuity:

$$\frac{E_{t_0,ssp_j} - E_{t_{-1},ssp_j}}{t_0 - t_{-1}} = 2a_j \left(\frac{t_0 - c_j}{b_j}\right) e^{-\frac{(t_0-c_j)^2}{b_j}} \tag{7}$$

The condition (7) equals the incremental ratio of SSP2.45 emission to the derivative value of the gaussian curve at the starting point of the optimization. This ensured a progressive transition in the emission reduction.

The suitable space took into account the economic, technical, and social elements evaluated by the IPCC. By analyzing IPCC AR6 scenarios and establishing the annual upper and lower limits of emissions, a feasible set of solutions was determined. The scenarios used consist of the five IMPs, together with a reference one known as CurPol:

- **CurPol — Current Policies**: Implementing existing climate policies (primarily as reported in Nationally Determined Contributions, NDCs), ignoring later goals and targets (e.g., 2030), Gradual Strengthening after 2030, and Gray COVID recovery.
- **GS – Gradual Strengthening**: Enforce the existing Nationally Determined Contributions (NDCs) until 2030, and thereafter establish a robust global framework that promotes synchronized and swift reduction of carbon emissions.
- **Neg – Net Negative Emissions**: An effective global climate policy framework aims to achieve emissions reductions below the Moderate Action scenario, as outlined in the IPCC AR6 report, or the GS route by 2030. Nevertheless, by prioritizing the long-term temperature objective, the magnitude of negative emissions intensifies, leading to a substantial "net global negative" after 2050 in order to achieve the 1.5 °C target after significant overshoot.
- **Ren — Renewables**: Rapid advancements in global climate policy, with a focus on promoting renewable energy legislation and providing financial support, while also reducing the use of negative-emission technologies. The rapid acceptance and advancement of renewable energy sources and technology, as well as the electrification of end-use applications.
- **LD — Low Demand**: Efficient global climate policies and financial incentives to decrease demand result in early reductions in emissions, abating supply-side decarbonization efforts.
- **SP — Shifting Pathways**: An efficient global climate strategy that prioritizes the Sustainable Development Goals

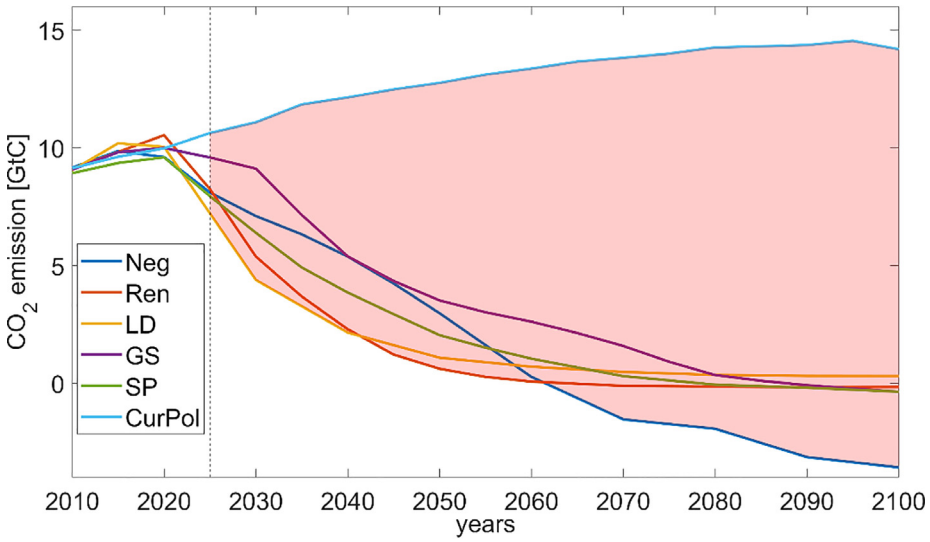

Fig. 2. IMP scenarios and CO_2 feasible region (red area).

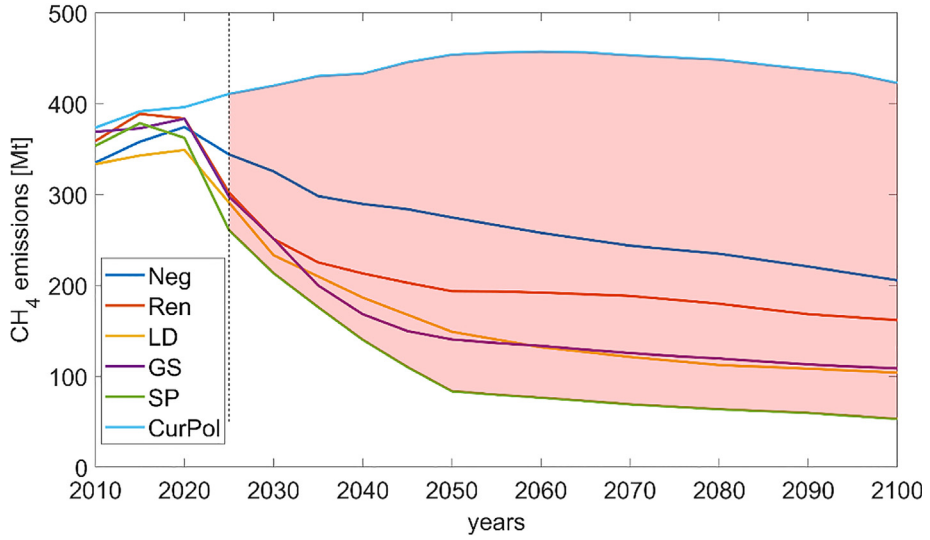

Fig. 3. IMP scenarios and CH_4 feasible region (red area).

(SDGs), such as reducing poverty and environmental preservation. Modifications improve sustainability, mitigate inequality, and achieve significant reductions in greenhouse gas emissions.

The feasible space of the possible solutions is highlighted in Fig. 2 for CO_2 and in Fig. 3 for CH_4.

2.2. FaIR climate model

FaIR (emissions-based impulse response model) simulates the climate system dynamics of the carbon cycle and other GHGs, taking into account the geological processes, the deep ocean, the ocean mixed layer, and the biosphere. Furthermore, it integrates external drivers such as solar and volcanic forcing, in addition to anthropogenic emissions of both GHGs and traditional pollutants like NH_3, NO_x, NMVOC, SO_x, black carbon (BC), and organic carbon (OC). FaIR provides valuable outputs such as GHG and pollutant concentrations, radiative forcing, and temperature, calculated as a difference from the pre-industrial era. FaIR emulates more complex models, which provide a more detailed description of the climate system with the decomposition of its elements shown in Fig. 4. The global climate is affected by several causes, including plate movements, solar activity, Earth's orbital location, and anthropogenic effects such as GHG emissions. These processes have very different timescales, and impact differently on the global system. FaIR, in its formulation, does not consider actual physical entities but indirectly takes into account the internal interactions of the climate system displayed in Fig. 4. In this work, acting on the land surface component by minimizing the temperature, the GHG emissions have been reduced, changing the atmospheric composition, and taking into account also the non-GHG species.

2.3. Non GHG emissions

It is well known that several sources emit both GHGs and air pollutants. For instance, vehicle emissions consist of CO_2, PM, and NO_x (Zimakowska-Laskowska & Laskowski, 2024). This is the same for heating processes, where SO_x, NO_x, and PM are emitted in addition to CO_2 (Ravina, Gamberini, Casasso, & Panepinto, 2020). Therefore, several mitigation strategies provide the opportunity to both enhance air quality and address climate change. These could include, for example, improvements

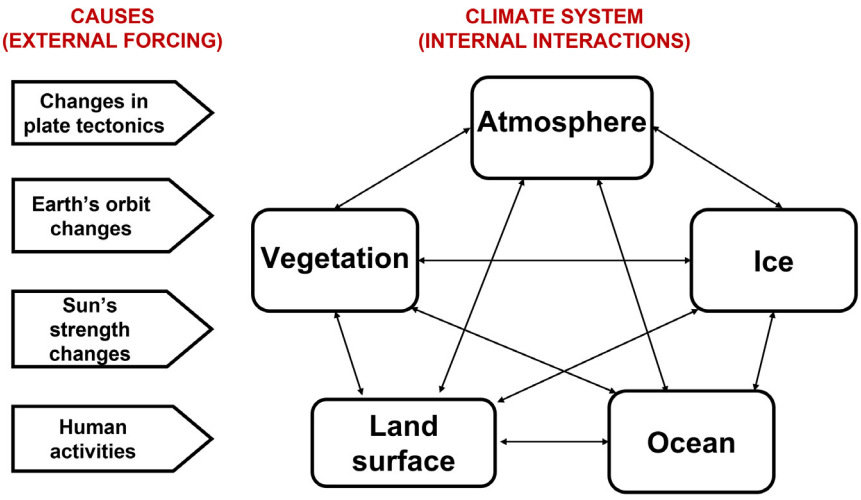

Fig. 4. The climate system and its components.

Table 1
Results for the different polynomial models to relate GHG with air pollutants using LD scenario.

	p1	p2	p3	p4	SSE	R^2	RMSE
CO_2 - SO_x	−0.0081	0.13	2.69	6.13	2.58	0.99	0.19
CO_2 - NMVOC	0.12	−0.75	8.36	76.47	131.72	0.99	1.34
CO_2 - NO_x	0.039	−0.24	2.99	16.72	10.38	0.99	0.38
CO_2 - PM	0.0037	0.18	0.46	12.31	12.52	0.99	0.41
CH_4 - NH_3	1.99×10^{-6}	-9.79×10^{-4}	0.21	16.24	10.67	0.99	0.41

in energy efficiency, as well as transitioning to wind or solar power, all of which result in overall emissions reduction (Schneidemesser et al., 2015; Williams, 2012). Thus, the relationships between GHG emissions and non-GHG air pollutants were estimated. Through the application of curve fitting methodology, CO_2 has been correlated with emissions of SO_x, NMVOC, NO_x, and PM, calculated as the sum of OC and BC. In addition, $CH_4$was related to NH_3, due to their significant interactions in agriculture (Malherbe et al., 2022). The relationships were constructed considering the IPCC IMP scenarios. The IMPs selected were chosen based on the shape of the optimization results in (Arrighini, Marchesi, Zecchi, & Volta, 2024). According to that, the exponential curve showed a similar trend to the LD scenario, while the gaussian function showed a trend comparable to the GS scenario. This is also confirmed by the similar value of the cumulative sum of emissions from 2025 to 2100. Two different approaches were used to determine the fitting: for the LD scenario, a third-degree polynomial function, and for the GS scenario, a cubic spline piecewise polynomial curve.

For LD scenario, the general equation of the polynomial form is the following:

$$y = p_1 x^3 + p_2 x^2 + p_3 x + p_4 \tag{8}$$

where p_1, p_2, p_3 and p_4 are the coefficients of the function, y are the emissions of traditional pollutants, and x are the emissions of GHG. The results are summarized in Table 1, where the sum of squares error (SSE), the coefficient R^2, and root mean square error (RMSE), are also indicated.

The polynomial results are shown in Fig. 5, which displays the different curves. Specifically, curves representing the relationships between CO_2 and SO_x, NO_x, VOC, and PM (a-d) are presented, along with the relationship between CH_4 and NH_3(e).

Fig. 6 displays the spline curves related to the different fittings with traditional pollutants related to the GS scenario. Fig. 6a-d shows the relationships between CO_2 and SO_x, NO_x, PM, and VOC, respectively, and CH_4 with ammonia is displayed in Fig. 6e.

2.4. Implementation

The optimization problem was implemented and solved utilizing the Sequential Quadratic Programming (SQP) algorithm for constrained nonlinear optimization in MATLAB®. The FaIR model was executed in MATLAB®, given its ability to use Python modules directly.

3. Results and discussion

This section presents quantitative outcomes obtained from the suggested methodology with different configurations identified by the following notation:

- For exponential reduction:
  - "EX" denotes the exponential reduction in (3).
  - The number following "EX" represents the starting year of the optimization (2025, 2030, 2035).
- For gaussian reduction:
  - "G" denotes the Gaussian pathway as expressed in (4).
  - The number following "G" represents the starting year of the optimization (2025, 2030, 2035).

In addition, OBJ1 refers to the solution using the objective function in (2), i.e., the total sum of temperatures from t_0 to 2100, and OBJ2 refers to the temperature value at 2100 (3).

3.1. OBJ1 solutions

The solutions of the optimization problem are in Table 2 where the different parameters for the reduction functions considered are given.

Fig. 7 shows the CO_2 emission for both gaussian (a) and exponential curves (b), inside the feasible region (red shaded

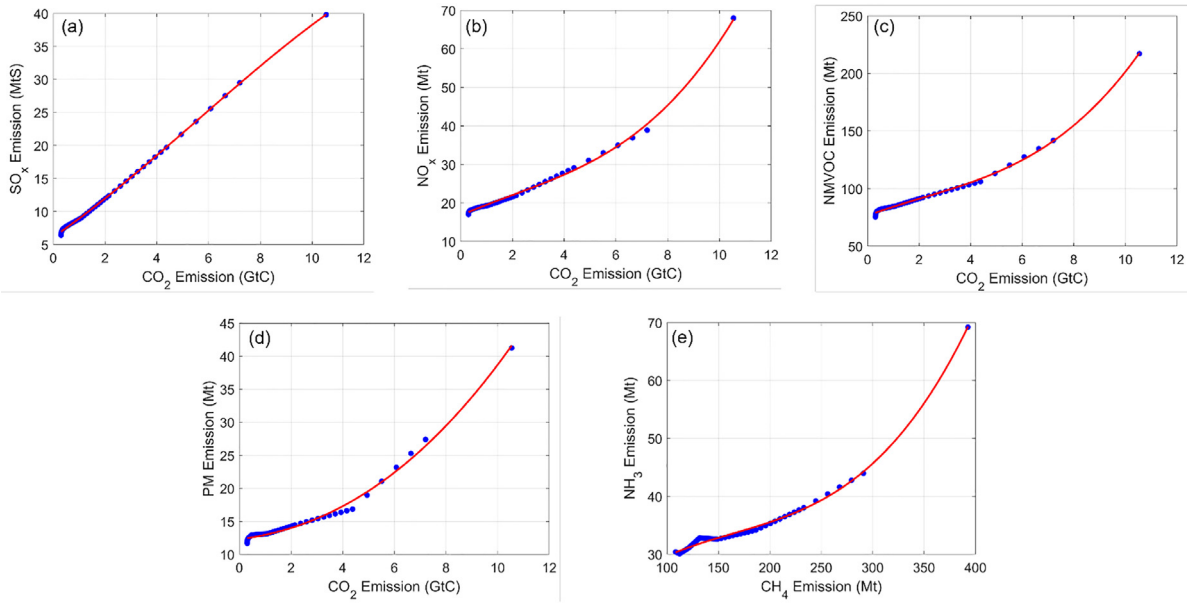

Fig. 5. Polynomial fitting results of the relationships between GHG species, CO_2 (a-d) and CH_4 (e), and traditional pollutants for LD scenario. CO_2 relationships include SO_x, NMVOC, NO_x, and PM while CH_4 is related only to ammonia.

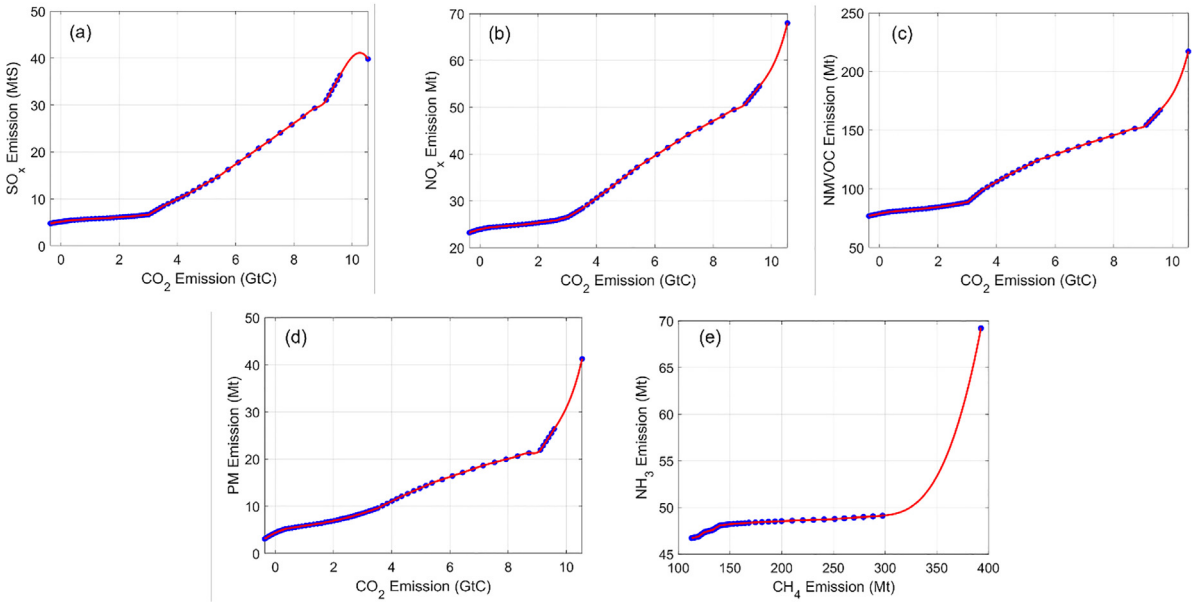

Fig. 6. Cubic spline fitting results of the relationships between GHG species, CO_2 (a-d) and CH_4 (e), and traditional pollutants for GS scenario. CO_2 relationships include SO_x, NMVOC, NO_x, and PM while CH_4 is related only to ammonia.

area). Fig. 7a displays the pathways for gaussian scenario. For G25 solution (orange line) CO_2 peaks at 38.67 Gt at the starting point, achieving net zero in 2070. At the end of the century, CO_2 will reach the value of −6.18 Gt. G30 solution (blue line) peaks at 40.27 Gt, with a net zero in 2075. Also, in this case CO_2 will reach negative values at the end of the century, by reaching −5.95 Gt. Finally, the purple line represents the G35 solution, with a peak of 41.19 Gt, and achieving the carbon neutrality in 2080. At the end of the century CO_2 will reach the value of −5.6 Gt.

In all cases the carbon neutrality was reached in 45 years, and the CO_2 emissions at 2100 reached negative values, which implies the necessary implementation of CCS technologies.

Exponential trajectories are shown in Fig. 7b. Depending on the starting year, the slope of the curve is more or less pronounced; in other words, the longer you wait to reduce emissions, the more you have to reduce them drastically to achieve the same result. Orange line represents the EX25 solution, which will gain the carbon neutrality between 2060 and 2070, and this is the same for EX30 (blue line), and EX35 (purple line). Moreover, EX25 and EX30 will have the final value of −1.29 Gt/y and −0.29 Gt/y, respectively, while EX35 will not reach negative value in 2100, but stabilize at a net carbon balance equal to zero.

The methane emissions are shown in Fig. 8. For the gaussian scenario (Fig. 8a), the G25 solution have the maximum value of 392.6 Mt/y with a reduction of about 86% until 2100 where a value of 53.6 Mt/y will be reached. G30 solution peaks at 398.3 Mt/y by achieving 53.6 Mt/y at the end of the century. Furthermore, G35 peaks at 392.8 Mt/y, by reaching the same value of the two previous results in 2100. In contrast, for exponential curves (Fig. 8b), all the emissions trajectories will have

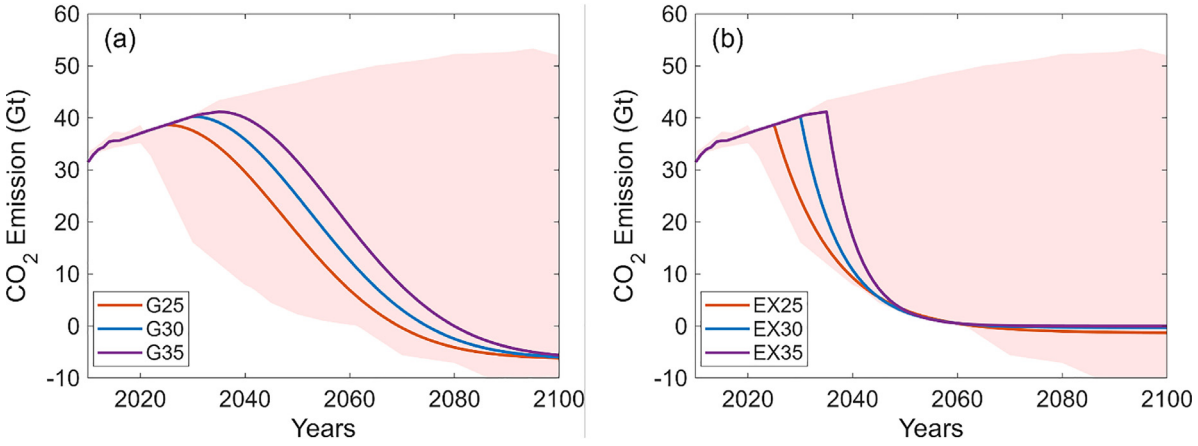

Fig. 7. CO_2 emission trajectories, solutions of the different decision problems for gaussian (a) and for exponential (b) curves in OBJ1.

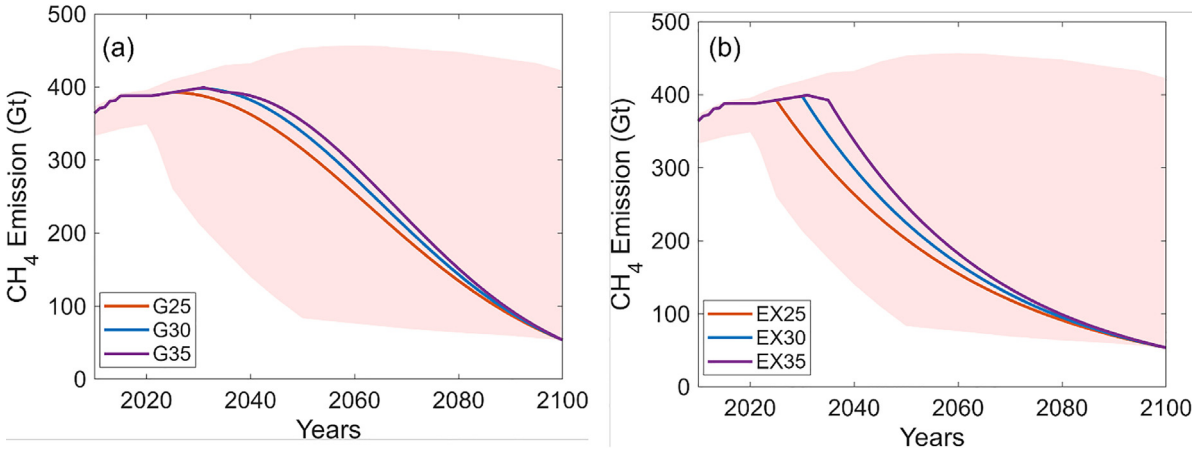

Fig. 8. CH_4 emission trajectories, solutions of the different decision problems, for gaussian (a) and for exponential (b) curves in OBJ1.

Table 2
Function coefficients for CO_2 and CH_4 for the different solutions of the decisional problem considering OBJ1 as objective function.

G25					**EX25**			
	a	**b**	**c**	**d**		**f**	**g**	**h**
CO_2	12.26	1000	2028.6	−1.72	CO_2	10.91	11.32	−0.37
CH_4	392.63	2826.7	2029.1	–	CH_4	392.6	37.7	–
G30					**EX30**			
	a	**b**	**c**	**d**		**f**	**g**	**h**
CO_2	12.70	1000	2033.5	−1.72	CO_2	11.06	7.69	−0.08
CH_4	398.31	2444.7	2033.5	–	CH_4	398.31	34.92	–
G35					**EX35**			
	a	**b**	**c**	**d**		**f**	**g**	**h**
CO_2	12.95	1000	2036.6	−1.72	CO_2	11.23	5.72	0
CH^4	392.78	2122.7	2030.5	–	CH_4	392.79	32.65	–

the final value of 53.67 Mt/y, but with a different curve slope. Here, it is more evident that different starting years imply more aggressive reduction policies. EX25 reduces emissions by about 86%, starting at 392.6 Mt/y, the same is true for EX35 but with a more aggressive reduction due to the later implementation. EX30 needs a slightly higher reduction of 88%, as it starts at 399 Mt/y.

The temperature anomaly plot is presented in Fig. 9. In this statement, since the system will not reach a saturated equilibrium, the overshoot is defined according to the IPCC report "Global Warming of 1.5 °C": the temporary exceedance of a specified 1.5 °C (Masson-Delmotte et al., 2018).

For the gaussian scenario (Fig. 9a) it is not just appropriate to talk about overshoots, simply because the exceedance was not temporary. G25 peaks at 1.92 °C in 2060, reaches 1.62 °C at the end of the century. G30 reaches 2 °C in 2070, with a final value of 1.74 °C. Lastly, G35 overtakes the limits of 2 °C by achieving 2.08 °C in 2070, with a decrease until 1.86 °C at the end of the century.

In the exponential scenario (Fig. 9b), all the solutions will reach a temperature less than or equal to 1.5 °C. Its EX25 (orange line) peaks at 1.65 °C in 2050, and it reaches 1.37 °C in 2100. EX30 reaches its maximum value of 1.73 °C in 2049, and it drops to 1.43 °C at the end of the century. EX35, has a maximum temperature value of 1.81 °C in 2049, achieving 1.5 °C in 2100.

3.2. OBJ2 solutions

The solutions of the optimization problem are in Table 3 where the different parameters for the reduction functions considered are given.

The second case study was the solution of (3), considering only the temperature value at the end of the century. The CO_2 emissions profile is shown in Fig. 10. For gaussian (Fig. 10a), the same results as OBJ1 were obtained. A little bit of a difference from OBJ1 can be observed for exponential decay (Fig. 10b), where all the solutions will achieve carbon neutrality at the same time in 2063. Furthermore, more negative emission values will be achieved at the end of the century: −5.41 Gt/y for EX25, −5.68 Gt/y for EX30, and −5.91 Gt/y for EX35, respectively.

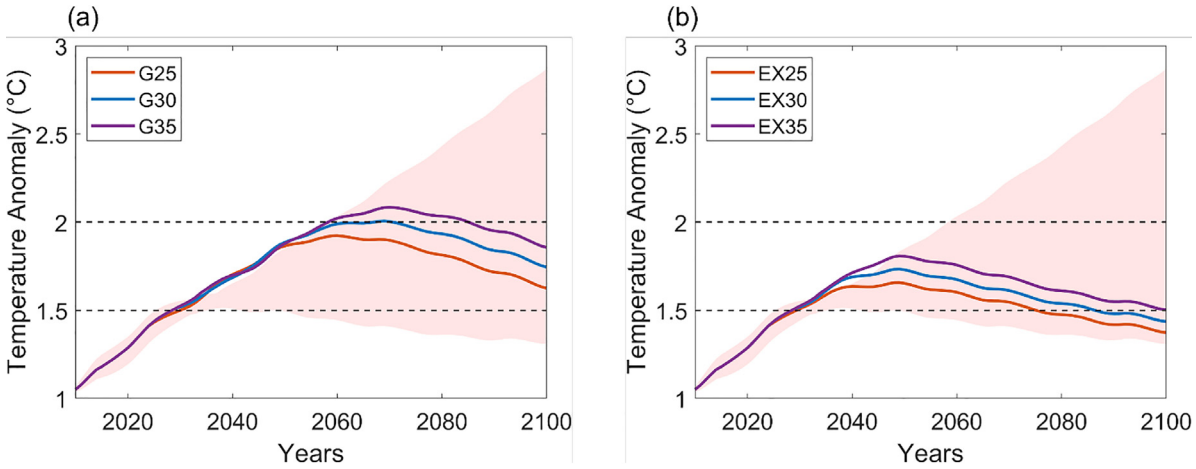

Fig. 9. Temperature anomaly of the optimized pathways gaussian (a) and exponential (b) in all considered configurations for the OBJ1. Results are compared to scenarios temperature trend (area in red).

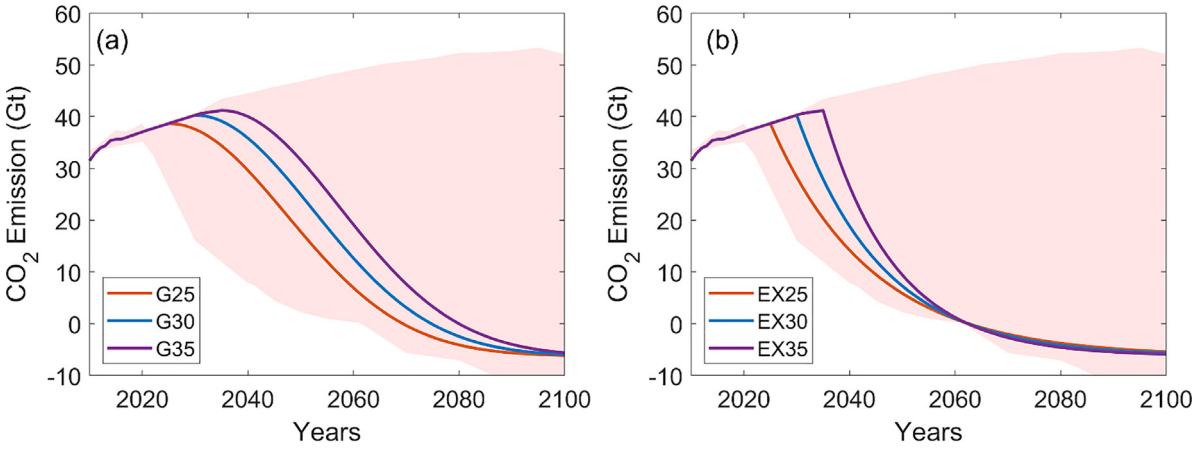

Fig. 10. CO_2 emission trajectories, solutions of the different decision problems, for gaussian (a) and exponential (b) curves in OBJ2.

Table 3
Function coefficients for CO_2 and CH_4 for the different solutions of the decisional problem considering OBJ2 as objective function.

G25					**EX25**				
	a	**b**	**c**	**d**		**f**	**g**	**h**
CO_2	12.26	1000	2028.6	−1.72	CO_2	12.26	19.10	−1.72
CH_4	392.63	2826.70	2029.1	–	CH_4	392.63	37.70	–
G30					**EX30**				
	a	**b**	**c**	**d**		**f**	**g**	**h**
CO_2	12.70	1000	2033.50	−1.72	CO_2	12.70	16.23	−1.72
CH_4	398.31	2444.70	2033.50	–	CH_4	398.31	34.92	–
G35					**EX35**				
	a	**b**	**c**	**d**		**f**	**g**	**h**
CO_2	12.95	1000	2036.60	−1.72	CO_2	12.95	13.56	−1.72
CH^4	392.78	2122.70	2030.50	–	CH_4	392.78	32.65	–

For CH_4 emissions, the same findings from OBJ1 were obtained, as shown in Fig. 11.

Lastly, the temperature anomalies over the century are displayed in Fig. 12. For the gaussian configuration (Fig. 12a), the same results as for OBJ1 were obtained. For the exponential setting (Fig. 12b), the same value of the temperature can be observed at the end of the century. However, here the solutions lead to a slightly higher overshoot with respect to the target of 1.5 °C. For EX25, the temperature reaches its maximum at 1.68 °C in 2050 and thereafter reaches 1.37 °C in 2100. Here, the maximum overshoot is about 0.18 °C, compared to 0.15 °C in OBJ1. Moreover, the anomaly exceeds 1.5 °C from 2030 to 2080, while for OBJ1 the overshoot ends five years earlier, in 2075. EX30 peaks at 1.76 °C in 2049, with a maximum overshoot of 0.26 °C and declining to 1.43 °C by the end of the century. Moreover, the overshoot lasts from 2030 to 2090, remaining at 1.5 °C for another four years and then decreasing. Finally, for EX35, the highest temperature value is projected to reach 1.82 °C in 2049 (0.32 °C of overshoot), with a target of hitting 1.5 °C by 2100. The same trend was obtained for OBJ1, with a maximum overshoot of 0.31 °C.

The results obtained were also compared in terms of the Integral of Emission (IoE) of CO_2, the cumulative sum of emissions from 2025 to 2100. Fig. 13 displays IoE values relative to OBJ1, compared with the IMP scenarios of IPCC. It is evident that as you advance the year in which emission reductions begin, this has a very important impact on them. The exponential pathways EX25, EX30, and EX35 have cumulative emission values of 371, 508, and 657 Gt, respectively. Taking 2025 as the base case, starting five years later implies an increase equal to 137 Gt, and an increase of 286 Gt if you start in 2035. This was not insignificant, considering that in this scenario, measures to lower emissions will be implemented with strong intensity, leading to a very rapid reduction.

For gaussian scenarios, G25 exhibits a cumulative value equal to 803 Gt, compared to 1076 and 1335 Gt for G30 and G35, respectively. Here, a bigger difference was achieved with respect

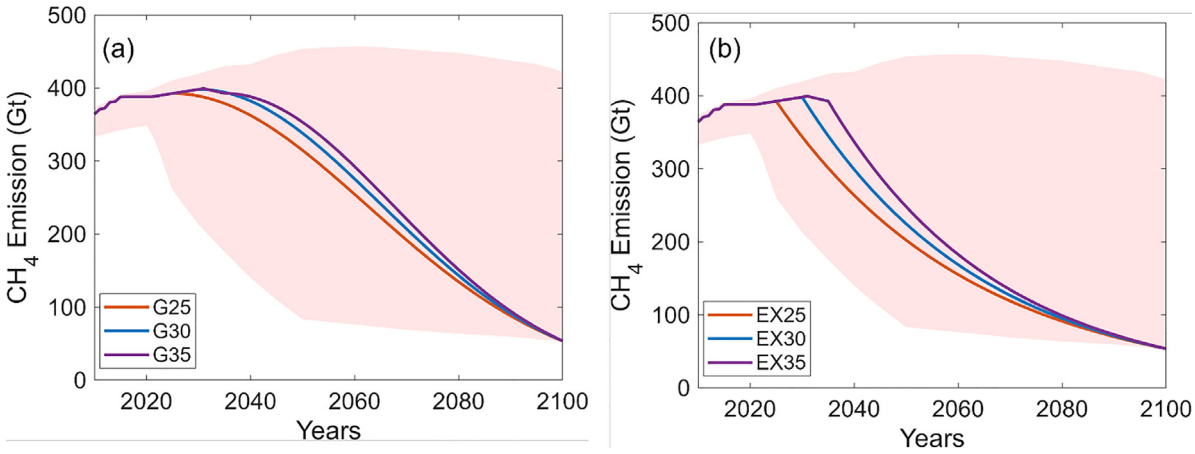

Fig. 11. CH_4 emission trajectories, solutions of the different decision problem, for gaussian (a) and exponential (b) curves in OBJ2.

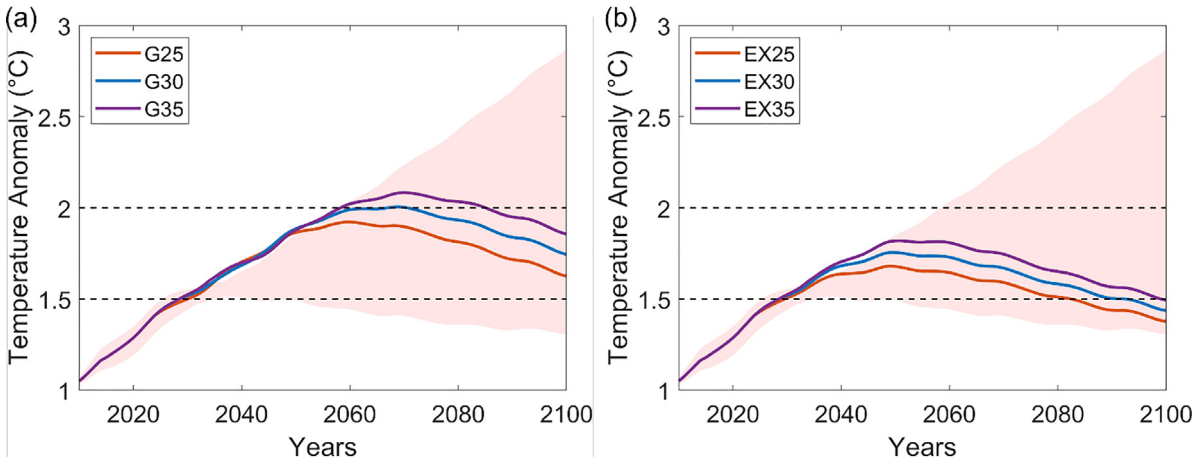

Fig. 12. Temperature anomaly of the optimized pathways, gaussian (a) and exponential (b), in all considered configurations for the OBJ2. Results are compared to the constraint scenarios temperature trend (area in red).

to the starting point. When you start in 2030, you will have a higher cumulative emission of 273 Gt, which will become 532 Gt if you start in 2035. Here, too, the starting year played a crucial role in climate change mitigation.

Regarding OBJ2, IoE results are shown in Fig. 14. For the gaussian pathway, the same results as for OBJ1 were attained. For exponential reduction, a little bit higher values were obtained for EX25 and EX30, where they exhibited a cumulative CO_2 emission of 387 and 519 Gt, respectively. On the other hand, for EX35, the cumulative value was equal to 647 Gt, 10 Gt less than obtained for OBJ1. In this case as well, the year in which reductions began played an essential role in efforts to mitigate climate change.

For the two case studies, the outcomes are summarized in Table 4 (OBJ1) and in Table 5 (OBJ2) for gaussian and exponential configurations. The two tables display the results in terms of the final temperature at the end of the century, the overshoot calculated as a difference between the maximum temperature anomaly and the target of 1.5 °C, and the year when carbon neutrality will be reached.

Table 4
Summary of the results for the different configurations of the decision problem related to OBJ1: temperature at the end of the century, maximum overshoot with respect to 1.5 °C, and the year of carbon neutrality.

	G25	G30	G35	E25	E30	E35
Final Temperature Anomaly (°C)	1.63	1.74	1.86	1.37	1.44	1.50
Overshoot (°C)	0.42	0.5	0.58	0.16	0.23	0.31
Carbon neutrality year	2070	2075	2080	2063	2065	2070

Table 5
Summary of the results for the different configurations of the decision problem related to OBJ2: temperature at the end of the century, maximum overshoot with respect to 1.5 °C, and the year of carbon neutrality.

	G25	G30	G35	E25	E30	E35
Final Temperature Anomaly (°C)	1.63	1.74	1.86	1.38	1.44	1.50
Overshoot (°C)	0.42	0.5	0.58	0.18	0.26	0.32
Carbon neutrality year	2070	2075	2080	2063	2063	2063

4. Conclusion

This research examined methods for reducing the impact of climate change through the use of optimization techniques. The study was addressed through the use of a top-down optimization approach. Unlike a bottom-up approach that prioritized finding the most efficient combination of actions, this approach optimizes CO_2 and CH_4 emission pathways for different policy factors, such as emission reduction propensity (gradual decay vs. drastic decrease), and GHG emission reduction start to determine their impact on temperature anomalies at the end of the century, and temperature anomaly overshoot. The decision problem was posed by changing the GHG emissions of CO_2 and CH_4, with the aim of minimizing the temperature anomaly from the pre-industrial

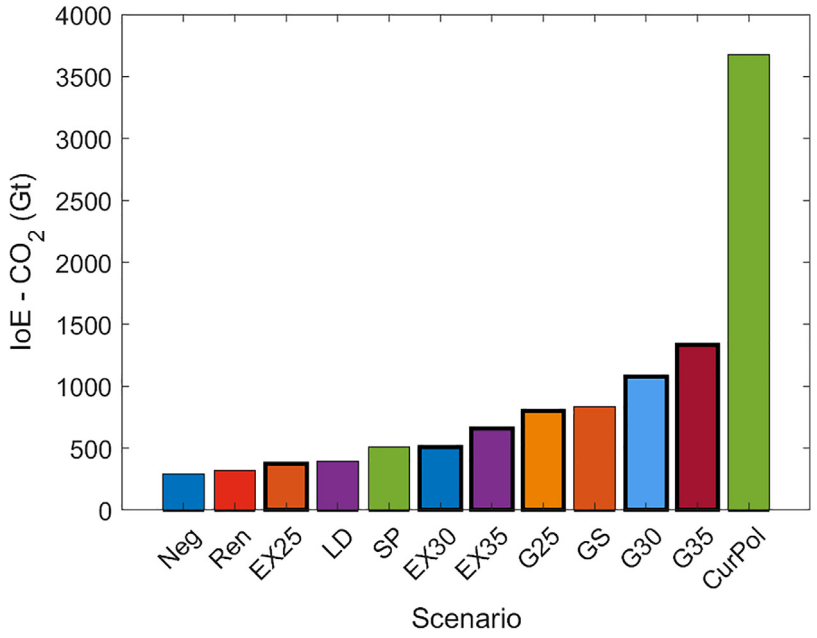

Fig. 13. Integral of CO_2 emissions for the optimal pathways compared to IMP scenarios for OBJ1.

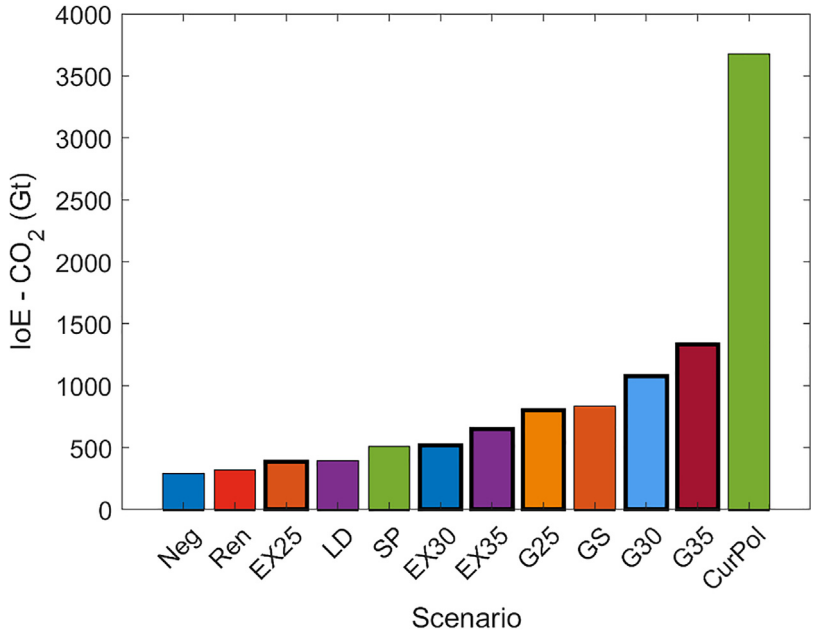

Fig. 14. Integral of CO_2 emissions for the optimal pathways compared to IMP scenarios for OBJ2.

era. Two different objective functions were considered: (i) the total sum of the temperature from 2025 to 2100, and (ii) only the value at the end of the century. In the first case, the occurrence of a temperature overshoot was constrained, while in the second one, it was unrestricted. The problem was investigated with the use of two distinct emission functions: a gaussian reduction approach and an exponential one. A Gaussian function represented a gradual abatement of the GHG emission, whereas an exponential curve reflected a more severe reduction. A progressive decrease in emissions over time distinguished the gaussian functional method, indicating the preservation of previous patterns. At first, the decrease in emissions was modest, which facilitates a gradual shift towards a lower level of emissions. It is a methodical and gradual strategy that aims to maintain a certain consistency with previous methods. On the other hand, the exponential method referred to a more quick and decisive decrease in initial emissions. Actions to decrease emissions will be carried out more aggressively, resulting in a faster reduction in the near term. However, attaining this road would involve concerted global coordination, robust policy promises, and constant monitoring and modification of emissions-reduction programs.

Furthermore, the starting point of the optimization was also changed in order to consider how this could impact the final results. In addition, the link between GHG and traditional pollutants was also considered to connect climate change to air quality policies. The relationships between CO_2 and other air pollutants such as SO_x, NMVOC, NO_x, and PM were achieved using a curve-fitting functional technique inside the optimization framework. A similar procedure was used to investigate the correlation between ammonia (NH_3) and CH_4.

Considering the sum of the temperatures as the objective function, gaussian solutions effectively ensured temperatures remained below the essential threshold of 2 °C. Comparing the results in terms of the starting year, one can see how these influenced the final temperature. G25 will reach 1.6 °C at 2100. Considering the starting point at 2030, the solution will achieve 1.74 °C. Finally, for the starting year at 2035, 1.86 °C will be reached at 2100. Moreover, this latter overtakes the 2 °C threshold, reaching 2.08 °C by the year 2070. Considering objective function 2, i.e., only the single temperature value at 2100, the results were exactly the same.

For the exponential approach, all solutions, with the exception of EX35, which achieved exactly 1.5 °C, stay below the temperature of 1.5 °C. Therefore, they completely outperformed the Gaussian pathways, making them more effective for climate change mitigation. EX25 exhibits a final temperature of 1.37 °C, in contrast to the 1.43 °C reached by the EX30 solution. The same trend as the Gaussian was observed in terms of economic consequences. Considering only the temperature value at 2100, the same results in terms of the final temperature were obtained. However, this was not the case for the different temperature pathways, where in all cases, there was a higher and longer temperature overshoot with respect to considering the total sum of the temperature as an objective function.

CRediT authorship contribution statement

Claudio Marchesi: Writing – original draft, Visualization, Investigation, Formal analysis, Data curation. **Michele Francesco Arrighini:** Writing – review & editing, Visualization, Validation, Software, Methodology, Investigation, Formal analysis, Data curation. **Laura Zecchi:** Writing – review & editing. **Marialuisa Volta:** Writing – review & editing, Supervision, Resources, Project administration, Methodology, Conceptualization.

Declaration of competing interest

The authors declare that they have no known competing financial interests or personal relationships that could have appeared to influence the work reported in this paper.

References

Ackerman, F., DeCanio, S. J., Howarth, R. B., & Sheeran, K. (2009). Limitations of integrated assessment models of climate change. *Climatic Change*, *95*(3–4), 297–315, 10.1007/S10584-009-9570-X/METRICS.

Anenberg, S. C., Dutton, A., Goulet, C. A., Swain, D. L., & van der Pluijm, B. (2019). Toward a resilient global society: Air, sea level, earthquakes, and weather. *Earth's Future*, *7*(8), 854–864. http://dx.doi.org/10.1029/2019EF001242.

Arrighini, M. F., Marchesi, C., Zecchi, L., & Volta, M. (2024). Optimal strategies for climate change mitigation. *IFAC-PapersOnLine*, *58*(2), 80–85. http://dx.doi.org/10.1016/J.IFACOL.2024.07.095.

Delbeke, J., Runge-Metzger, A., Slingenberg, Y., & Werksman, J. (2019). The paris agreement. In *Towards a climate-neutral europe: curbing the trend* (pp. 24–45). http://dx.doi.org/10.4324/9789276082569-2/PARIS-AGREEMENT-JOS-DELBEKE-ARTUR-RUNGE-METZGER-YVON-SLINGENBERG-JAKE-WERKSMAN.

Duan, H., Zhang, G., Wang, S., & Fan, Y. (2019). Robust climate change research: a review on multi-model analysis. *Environmental Research Letters*, *14*(3), Article 033001. http://dx.doi.org/10.1088/1748-9326/AAF8F9.

Eghweree, C. O., & Imuetinyan, F. O. (2019). Africa and the climate change diplomacy. *Journal of Sustainable Development*, *12*(2), 101. http://dx.doi.org/10.5539/JSD.V12N2P101.

Fricko, O., Parkinson, S. C., Johnson, N., Strubegger, M., Vliet, M. T. Van, & Riahi, K. (2016). Energy sector water use implications of a 2 °c climate policy. *Environmental Research Letters*, *11*(3), Article 034011. http://dx.doi.org/10.1088/1748-9326/11/3/034011.

Hasegawa, T., Fujimori, S., Ito, A., Takahashi, K., & Masui, T. (2017). Global land-use allocation model linked to an integrated assessment model. *Science of the Total Environment*, *580*, 787–796. http://dx.doi.org/10.1016/J.SCITOTENV.2016.12.025.

Hejazi, M., Edmonds, J., Clarke, L., Kyle, P., Davies, E., Chaturvedi, V., Wise, M., Patel, P., Eom, J., Calvin, K., Moss, R., & Kim, S. (2014). Long-term global water projections using six socioeconomic scenarios in an integrated assessment modeling framework. *Technological Forecasting and Social Change*, *81*(1), 205–226. http://dx.doi.org/10.1016/J.TECHFORE.2013.05.006.

Howells, M., Hermann, S., Welsch, M., Bazilian, M., Segerström, R., Alfstad, T., Gielen, D., Rogner, H., Fischer, G., Van Velthuizen, H., Wiberg, D., Young, C., Roehrl, R. Alexander, Mueller, A., Steduto, P., & Ramma, I. (2013). Integrated analysis of climate change, land-use, energy and water strategies. *Nature Climate Change*, *3*(7), 621–626. http://dx.doi.org/10.1038/nclimate1789.

Leach, N. J., Jenkins, S., Nicholls, Z., Smith, C. J., Lynch, J., Cain, M., Walsh, T., Wu, B., Tsutsui, J., & Allen, M. R. (2021). FaIRv2.0.0: A generalized impulse response model for climate uncertainty and future scenario exploration. *Geoscientific Model Development*, *14*(5), http://dx.doi.org/10.5194/GMD-14-3007-2021.

Malherbe, L., German, R., Couvidat, F., Zanatta, L., Blannin, L., James, A., Lètinois, L., Schucht, S., Berthelot, B., & Raoult, J. (2022). Emissions of ammonia and methane from the agricultural sector emissions from livestock farming. https://www.eionet.europa.eu/etcs/all-etc-reports.

Masson-Delmotte, V., Zhai, P., Pörtner, H.-O., Roberts, D., Skea, J., Shukla, P. R., Pirani, A., Moufouma-Okia, W., Péan, C., Pidcock, R., Connors, S., Matthews, J. B. R., Chen, Y., Zhou, X., Gomis, M. I., Lonnoy, E., Maycock, T., Tignor, M., & Waterfield, T. (2018). Global warming of 1.5 °c an IPCC special report on the impacts of global warming of 1.5 °c above pre-industrial levels and related global greenhouse gas emission pathways, in the context of strengthening the global response to the threat of climate change, sustainable development, and efforts to eradicate poverty. http://dx.doi.org/10.1017/9781009157940.

Mouratiadou, I., Biewald, A., Pehl, M., Bonsch, M., Baumstark, L., Klein, D., Popp, A., Luderer, G., & Kriegler, E. (2016). The impact of climate change mitigation on water demand for energy and food: An integrated analysis based on the shared socioeconomic pathways. *Environmental Science & Policy*, *64*, 48–58. http://dx.doi.org/10.1016/J.ENVSCI.2016.06.007.

Rafaj, P., Kiesewetter, G., Krey, V., Schoepp, W., Bertram, C., Drouet, L., Fricko, O., Fujimori, S., Harmsen, M., Hilaire, J., Huppmann, D., Klimont, Z., Kolp, P., Reis, L. Aleluia, & Van Vuuren, D. (2021). Air quality and health implications of 1.5 °C–2 °C climate pathways under considerations of ageing population: a multi-model scenario analysis. *Environmental Research Letters*, *16*(4), Article 045005. http://dx.doi.org/10.1088/1748-9326/ABDF0B.

Ravina, M., Gamberini, C., Casasso, A., & Panepinto, D. (2020). Environmental and health impacts of domestic hot water (DHW) boilers in urban areas: A case study from turin, NW Italy. *International Journal of Environmental Research and Public Health*, *17*(2), http://dx.doi.org/10.3390/IJERPH17020595.

Riahi, K., van Vuuren, D. P., Kriegler, E., Edmonds, J., O'Neill, B. C., Fujimori, S., Bauer, N., Calvin, K., Dellink, R., Fricko, O., Lutz, W., Popp, A., Cuaresma, J. C., S, K. C., Leimbach, M., Jiang, L., Kram, T., Rao, S., Emmerling, J., ... Tavoni, M. (2017). The shared socioeconomic pathways and their energy, land use, and greenhouse gas emissions implications: An overview. *Global Environmental Change*, *42*, 153–168. http://dx.doi.org/10.1016/J.GLOENVCHA.2016.05.009.

R.J. Nicholls, Z., Meinshausen, M., Lewis, J., Gieseke, R., Dommenget, D., Dorheim, K., Fan5, C. S., Fuglestvedt, J. S., Gasser, T., Goluke, U., Goodwin, P., Hartin, C., P. Hope, A., Kriegler, E., J. Leach, N., Marchegiani, D., A. McBride, L., Quilcaille, Y., Rogelj, J., ... Xie, Z. (2020). Reduced complexity model intercomparison project phase 1: Introduction and evaluation of global-mean temperature response. *Geoscientific Model Development*, *13*(11), 5175–5190. http://dx.doi.org/10.5194/GMD-13-5175-2020.

Saunois, M., R. Stavert, A., Poulter, B., Bousquet, P., G. Canadell, J., B. Jackson, R., A. Raymond, P., J. Dlugokencky, E., Houweling, S., K. Patra, P., Ciais, P., K. Arora, V., Bastviken, D., Bergamaschi, P., R. Blake, D., Brailsford, G., Bruhwiler, L., M. Carlson, K., Carrol, M., ... Zhuang, Q. (2020). The global methane budget 2000–2017. *Earth System Science Data*, *12*(3), 1561–1623. http://dx.doi.org/10.5194/ESSD-12-1561-2020.

Sherwood, S. C., Webb, M. J., Annan, J. D., Armour, K. C., Forster, P. M., Hargreaves, J. C., Hegerl, G., Klein, S. A., Marvel, K. D., Rohling, E. J., Watanabe, M., Andrews, T., Braconnot, P., Bretherton, C. S., Foster, G. L., Hausfather, Z., von der Heydt, A. S., Knutti, R., Mauritsen, T., ... Zelinka, M. D. (2020). An assessment of earth's climate sensitivity using multiple lines of evidence. *Reviews of Geophysics*, *58*(4), Article e2019RG000678. http://dx.doi.org/10.1029/2019RG000678.

Shukla, P. R., Skea, J., Slade, R., Al Khourdajie, A., van Diemen, R., McCollum, D., Pathak, M., Some, S., Vyas, P., Fradera, R., Belkacemi, M., Hasija, A., Lisboa, G., & Luz, S. (2023). Climate change 2022 - mitigation of climate change. In Intergovernmental Panel on Climate Change (IPCC) (Ed.), *Contribution of working group III to the sixth assessment report of the intergovernmental panel on climate change*. Cambridge University Press, http://dx.doi.org/10.1017/9781009157926.

Smith, C. J., Forster, P. M., Allen, M., Leach, N., Millar, R. J., Passerello, G. A., & Regayre, L. A. (2018). FAIR v1.3: A simple emissions-based impulse response and carbon cycle model. *Geoscientific Model Development*, *11*(6), 2273–2297. http://dx.doi.org/10.5194/GMD-11-2273-2018.

Von Schneidemesser, E., Monks, P. S., Allan, J. D., Bruhwiler, L., Forster, P., Fowler, D., Lauer, A., Morgan, W. T., Paasonen, P., Righi, M., Sindelarova, K., & Sutton, M. A. (2015). Chemistry and the linkages between air quality and climate change. *Chemical Reviews*, *115*(10), 3856–3897. http://dx.doi.org/10.1021/ACS.CHEMREV.5B00089/ASSET/IMAGES/LARGE/CR-2015-00089V_0013.JPEG.

Williams, M. (2012). Tackling climate change: what is the impact on air pollution? *Carbon Management*, *3*(5), 511–519. http://dx.doi.org/10.4155/CMT.12.49.

Zimakowska-Laskowska, M., & Laskowski, P. (2024). Comparison of pollutant emissions from various types of vehicles. *Combustion Engines*, http://dx.doi.org/10.19206/CE-181193.